Active Site-Directed Inhibitors of Prolyl Oligopeptidase Abolishes its Conformational Dynamics

Abraham López,[a, b] Fátima Herranz-Trillo,[c] Martin Kotev,[d] Margarida Gairí,[e] Víctor Guallar,[d, f] Pau Bernadó,[c] Oscar Millet,[g] Teresa Tarragó,[a, h] and Ernest Giralt*[a, b]

Abstract: Deciphering conformational dynamics is crucial for understanding the biological functions of proteins and for designing compounds targeting them. In particular, providing an accurate description of μs-ms motions opens up the opportunity for regulating protein-protein interactions (PPIs) by modulating dynamics of one interacting partner. Here we analyzed the conformational dynamics of prolyl oligopeptidase (POP) and the effects of active site-directed inhibitors on the dynamics. For this purpose, we used an integrated structural biology approach based on NMR spectroscopy and SAXS experiments complemented by MD simulations. Our results found that POP is in a slow equilibrium in solution between open and closed conformations, and that inhibitors effectively prevented this equilibrium by stabilizing the enzyme in a closed conformation.

Dynamics is an essential component for the biological functions of proteins.[1] Therefore, the characterization of protein motions is fundamental for developing therapeutic compounds that may modulate conformational dynamics of their targets. Considering the emergent therapeutic focus on protein-protein interactions (PPIs),[2] modulating μs-ms dynamics opens up a valuable opportunity for regulating the affinity and specificity of recognition between flexible proteins.[3] Hence, the design of compounds that modify conformational dynamics stand as a promising strategy for controlling PPI networks involved in pathogenic mechanisms.

Prolyl Oligopeptidase (POP) is an 81-KDa monomeric serine peptidase that hydrolyzes short peptides at the carboxyl side of proline.[4] The structure of POP is divided in two domains, namely α/β-hydrolase and the β-propeller, which are linked by a pair of hinge polypeptide chains. X-ray structures of the mammalian enzyme shows that the α/β-hydrolase and β-propeller are packed together in a closed conformation (Figure 1 A).[5] However, the crystallization of two bacterial POPs showing a large-scale hinge separation between domains[6] (Figure 1 B) suggested that the mammalian enzyme might undergo interdomain flexibility.[7] In this direction, two studies based on ^{15}N line broadening NMR experiments[8] and X-ray crystallography combined with MD simulations[9] strongly supported that POP is a highly flexible enzyme, but several fundamental aspects concerning the conformational landscape of POP in solution and the effects of inhibitors are largely unknown.

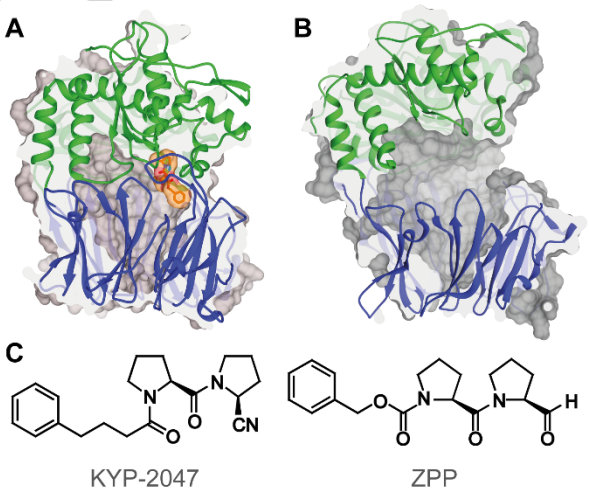

Figure 1. A) Porcine POP in the closed conformation (PDB ID: 1QFS[5]), covalently bound to the active site-directed inhibitor ZPP (orange). The α/β-hydrolase is shown in green and the β-propeller in blue. B) *Aeromonas punctata* POP in the open conformation (PDB ID: 3IUJ[6a]), colored following the same code as in A). C) Chemical structures of ZPP and KYP-2047 inhibitors.

The *in vivo* role of POP is related to synaptic functions and neuronal development. In this regard, it has been found that POP interacts with the intrinsically disordered proteins α-synuclein and GAP-43.[10] Recent studies have demonstrated that the direct interaction between POP and α-synuclein, the protein involved in the development of Parkinson's disease, accelerates the aggregation of α-synuclein *in vitro* and in cells.[11] Interestingly, KYP-2047,[12] a covalent active site-directed inhibitor of POP (Figure 1 C) effectively reduce aggregation *in vitro* and *in vivo*.[11a, 13] Further experiments have shown that this reduction is a consequence of an increased *in vivo* clearance of aggregated forms of α-synuclein promoted by POP inhibition.[13b]

[a] Dr. A. López, Dr. T. Tarragó, Prof. E. Giralt
Chemistry and Molecular Pharmacology Program
Institute for Research in Biomedicine, The Barcelona Institute of Science and Technology
Baldiri Reixac 10, 08028, Barcelona, Spain
E-mail: ernest.giralt@irbbarcelona.org
[b] Dr. A. López, Prof. E. Giralt
Department of Organic Chemistry
University of Barcelona
Martí i Franquès, 1-11, 08028, Barcelona, Spain
[c] F. Herranz-Trillo, Dr. Pau Bernadó
Centre de Biochimie Structurale
INSERM U1054, CNRS UMR 5048, Université de Montpellier 1 and 2
29 rue de Navacelles, 34090, Montpellier, France
[d] Dr. M. Kotev, Dr. V. Guallar
Joint BSC-CRG-IRB Research Program in Computational Biology
Barcelona Supercomputing Center
Jordi Girona 31, 08034, Barcelona, Spain
[e] Dr. M. Gairí
NMR Facility
Scientific and Technological Centers University of Barcelona (CCiTUB)
Baldiri Reixac 10, 08028, Barcelona, Spain
[f] Dr. V. Guallar
Institució Catalana de Recerca i Estudis Avançats (ICREA)
Passeig Lluís Companys 23, 08010, Barcelona, Spain
[g] Dr. O. Millet
Structural Biology Unit
CIC bioGUNE
Parque Tecnológico de Vizcaya, Ed. 800, 48160 Derio, Spain
[h] Dr. T. Tarragó
Iproteos, S L
Barcelona Science Park, Baldiri Reixac 10, 08028, Barcelona, Spain

Supporting information for this article is given via a link at the end of

Nevertheless, the lack of knowledge on the conformational dynamics of POP and the effects of inhibitors represents a major impediment for exploring the mechanisms underlying POP-mediated aggregation of α-synuclein. For this reason, here we have analysed in detail the conformational equilibrium of POP in solution and how it is affected by the binding of active-site directed inhibitors. For this purpose, we have combined the capacity of NMR spectroscopy to describe dynamic events at atomic resolution[14] with the potential of SAXS experiments complemented with MD simulations to probe large-scale structural fluctuations in solution.[15]

Conformational dynamics of POP in the time scale of μs-ms was analyzed by methyl-TROSY ^{13}C-^{1}H multiple quantum relaxation dispersion (RD) experiments[16] using selective labeling of methyl positions of methionine residues.[17] Methionine methyl groups are excellent reporters of structure and dynamics due to simplified spectra and the high sensitivity and resolution achieved using the TROSY effect.[18] To assign the methyl-TROSY spectrum, we took site-directed mutagenesis approach (see Supporting Information). In order to eliminate the contribution of dipolar relaxation from surrounding protons in the effective transverse relaxation rates ($R_{2,eff}$),[16, 18] we produced a highly deuterated [methyl-^{13}C]-methionine-labeled POP. For this purpose, methionine auxotrophic *E.coli* cells were supplemented with [methyl-^{13}C]-L-methionine (2, 3, 3, 4, 4, - d_5) in a highly deuterated expression medium. This methionine isotopomer was chemically synthesized in order to achieve high deuterium content in non-labeled positions, especially in β and γ positions (see Supporting Information). Interestingly, RD experiments of free POP showed intense decay curves for most methionine signals (Figure 2, red), providing robust signatures for the pervasive μs-ms dynamics of the free enzyme. Estimated values of the exchange parameters were extracted by fitting the RD data to a two-state mode.l[16] k_{ex} values obtained from fitting of RD data were comprised between 38 s^{-1} to 167 s^{-1}, with a population between exchanging states around 50% (Table 1). Figure 3 A shows that highest amplitude motions were localized in the α/β-hydrolase domain.

Afterwards, the effects of binding of the covalent active site-directed inhibitors benzyloxycarbonyl-prolyl-prolinal (ZPP, Figure 1 C)[19] and KYP-2047 on POP conformational dynamics were examined. Extensive changes in the methyl-TROSY spectra of inhibited POP indicated large-scale conformational rearrangements upon inhibitor binding, which predominantly affected the α/β-hydrolase (Figures 3 B and S3). Remarkably, RD experiments of inhibited POP revealed that inhibition caused dramatic effects in μs-ms dynamics. The decay in the RD profiles of methionine residues was effectively abolished (Figure 2, blue), indicating that the binding of inhibitors totally prevented the conformational dynamics of POP.

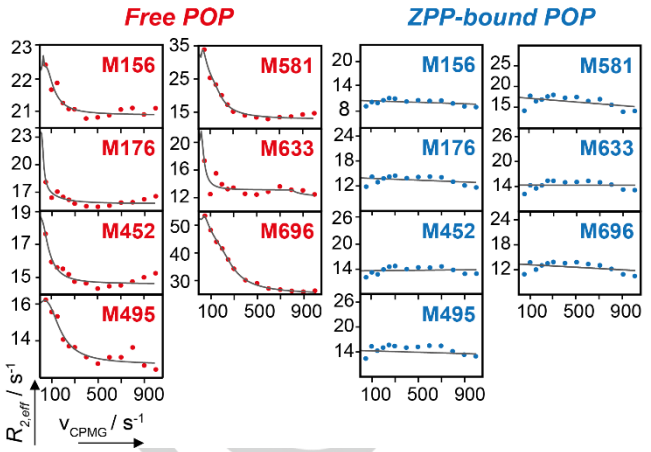

Figure 2. Multiple quantum RD experiments of highly deuterated [methyl-^{13}C]-methionine-labeled POP. RD profiles of methionine residues of free POP and ZPP-bound POP are shown in red and blue, respectively; solid lines correspond to the best fits of the data to a two-state model.

Table 1. Summary of exchange parameters of free POP extracted from the fitting of multiple quantum RD data.

Methionine	k_{ex} (s^{-1})	p_B (%)	Methionine	k_{ex} (s^{-1})	p_B (%)
156	45 ± 7	49	581	52 ± 18	46
176	50 ± 9	49	633	50 ± 13	50
452	38 ± 11	51	696	112 ± 14	47
495	167 ± 21	45			

In order to unravel the structural aspects of the conformational dynamics of POP and the effects of inhibitor binding, we used SAXS, a highly versatile technique that probes molecular structure at low resolution in solution.[15] Free and ZPP-bound POP samples were analyzed using an online gel filtration chromatography coupled to SAXS in order to eliminate the interference of protein aggregates (Figure S4 in the Supporting Information). In the two cases, scattering profiles of eluted monomer species presented high spectral homogeneity as determined by singular value decomposition (see Supporting Information). Subsequently, these profiles were averaged to obtain the corresponding high-quality scattering profiles, which showed no signatures of interparticle interactions or radiation damage (see Figures 4 A and S5 in the Supporting Information). Afterwards, the overall size of particles in solution was evaluated by extracting the radius of gyration (R_g). Comparison of R_g of free and inhibited POP disclosed significant structural differences between the two forms of the enzyme (R_g of 28.50 ± 0.06 Å vs. 27.40 ± 0.06 Å, respectively). In turn, the pair-distance distribution functions (*P(r)* Figure 4 B) of free and inhibited POP revealed significant differences in the global shape. *P(r)* function of free POP yielded a multimodal distribution with a maximum dimension (D_{max}) of 86 ± 3 Å, while

ZPP-bound POP showed a Gaussian-like distribution of smaller D_{max} (81 ± 3 Å).

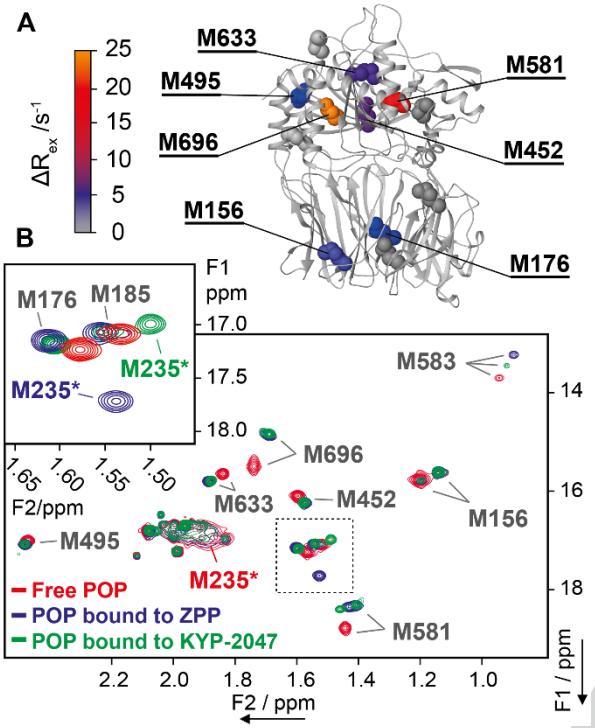

Figure 3. A) Structure distribution of *ΔRex* values obtained by multiple quantum RD experiments of free POP. B). Assigned methyl-TROSY spectrum of free POP (red) overlaid with the spectra of POP bound to ZPP (blue) and of POP bound to KYP-2047 (green). Enlarged view of the boxed region shows that the signal of methionine 235 (marked with an asterisk) is strongly sensitive to the binding of active site-directed inhibitors.

To ultimately assess the conformational equilibrium of POP and the structural consequences of inhibitor binding, we took advantage of the ensemble optimization method (EOM),[20] a procedure that optimizes a sub-ensemble of structures from a large pool of model structures using the experimental scattering profile as a driving force. To obtain a large pool of models sampling a broad conformational space, we performed MD simulations starting from the crystallographic structure of POP in the closed conformation and the porcine homology model of *Aeromonas punctata* POP in the open conformation (see Supporting Information). Hence, the EOM of free and ZPP-bound POP provided sub-ensembles of conformations that collectively described the experimental scattering profiles with excellent fit (Figures 4 A and S6 in the Supporting Information). Structures of free POP selected by the EOM consisted of 55% of fully open and 45% of closed conformations (Figure 4 C, red). These conformational populations are in agreement with those extracted from the fitting of RD data, providing a cross-validation between the two approaches. Theoretical averaged R_g of selected open structures was 30.50 ± 0.08 Å, whereas in the closed structures this value was 27.35 ± 0.07 Å, being fully compatible with the experimental R_g of free POP (28.50 ± 0.06 Å). In contrast, selected structures of POP bound to ZPP consisted exclusively of closed conformations resembling the X-ray structure of POP covalently bound to ZPP (Figure 4 C, blue). Theoretical averaged R_g of selected structures of inhibited POP also was in good agreement with the experimental value (R_g values of 27.23 ± 0.01 Å vs. 27.40 ± 0.06 Å, respectively).

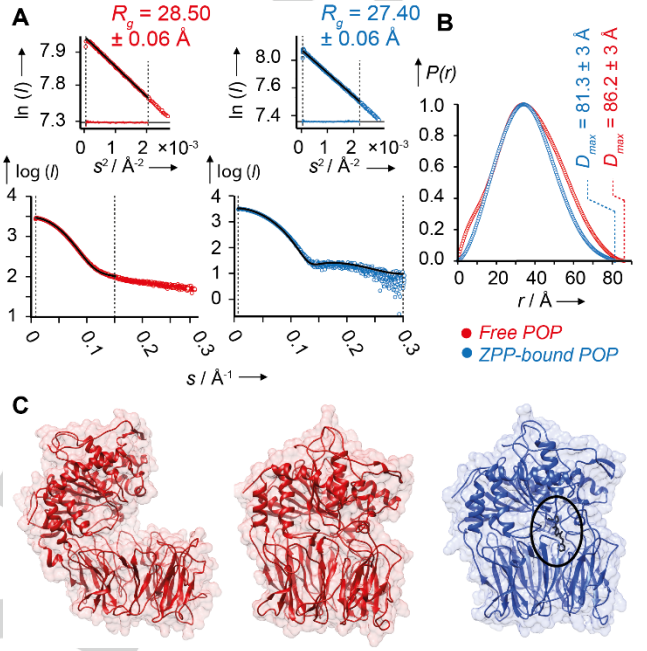

Figure 4. SAXS experiments of free and inhibited POP. A) Averaged scattering profiles of free POP (red) and ZPP-bound POP (blue). Insets show R_g values and Guinier plots, which confirms the absence of interparticle interactions and radiation damage. The theoretical scattering profile obtained by the EOM is shown in black. B) *P(r)* distribution of free POP (red) and ZPP-bound POP (blue). Dotted lines shows the corresponding maximum dimensions (D_{max}), which reflects the bigger size of free POP. C) Structures of POP selected by the EOM. Representative open and closed structures of free POP are shown in red, and representative closed conformation of POP covalently bound to ZPP is shown in blue; inhibitor is marked by a black circle.

In summary, the integrated approach combining NMR spectrometry and SAXS experiments complemented by MD simulations have demonstrated that POP is a highly dynamic enzyme in the ms time scale, showing an equilibrium between open and closed conformations. In turn, we have shown that the binding of active site-directed inhibitors effectively impedes the conformational exchange by stabilizing POP in a closed conformation. According to these results, it can be therefore proposed that µs-ms conformational dynamics of POP causes significant fluctuations in the configuration of the surface(s) involved in molecular recognition events. Hence, stabilizing the POP in a closed conformation by inhibitors would cause substantial alterations on the affinity and specificity of the native PPIs of the enzyme. We speculate that this mechanism could represent a central feature for the reversibility of POP-mediated aggregation of α-synuclein induced by active site-directed POP inhibitors which has been reported in the literature.[11, 13] Overall, the results presented here open the way for designing novel

POP inhibitors conceived as conformational modulators able to regulate the native interactome of the enzyme.

Experimental Section

Cells were purchased from Novagen, chemicals from Sigma-Aldrich, and deuterated chemicals from Cambridge Isotope Laboratories. Affinity and size exclusion chromatography columns were from GE Healthcare Life Sciences.

Expression of POP and [methyl-^{13}C]-methionine-labeled POP: POP was expressed in *Escherichia coli* BL21 (DE3) cells using pET-11 plasmid containing the human POP gene, following a standard protocol.[21] HisTag was removed by digestion with TEV protease, and POP was purified in a Superdex 200 HiLoad column before performing the experiments. For the [methyl-^{13}C]-methionine-labeled POP, auxotrophic *E. coli* B834(DE3) cells were grown in minimal media containing 80 mg/l of [methyl-^{13}C]-L-methionine. Purification was performed as described previously. In the case of highly deuterated [methyl-^{13}C]-methionine-labeled POP, auxotrophic *E.coli* B834(DE3) cells were transformed with pETM-10 plasmid containing the human POP gene. Cells were grown in deuterated minimal medium supplemented with 2 g/l D-glucose (1, 2, 3, 4, 5, 6, 6 – d_7) and 50 mg/l [methyl-^{13}C]-L-methionine (2, 3, 3, 4, 4, - d_5), synthesized as described in the Supporting Information. HisTag cleavage was not performed in this case. The binding of ZPP and KYP-2047 inhibitors was carried out by drying an aliquot of 10 equivalents of the inhibitor dissolved in 1,4-dioxane with a soft stream of N_2 in a small glass tube. Afterwards, POP sample was added to the tubes containing the dried inhibitor aliquot and incubated for 20 min at room temperature.

NMR experiments and fitting of RD data: All NMR experiments were performed at 25°C in a Bruker 800 MHz Avance III spectrometer equipped with a cryoprobe. POP samples comprised between 200 and 250 µM in Tris d_{11}-HCl 50 mM pH 8, NaCl 20 mM, DTT d_6 1 mM, NaN_3 0.03%, and 100% D_2O buffer. ^{1}H-^{13}C methyl-TROSY HMQC experiments used the pulse sequence described by Tugarinov *et al.*[18] Spectra comprised 128, 512 data points (F1, F2), with 240 scans per FID separated by an interscan delay of 1.5 s. ^{1}H-^{13}C methyl-TROSY HMQC RD experiments[16] used a CPMG element of 40 ms, with 0, 2, 4, 6, 8, 10, 12, 16, 20, 24, 28, 32, 36 and 40 randomly ordered inversion pulses. Spectra were recorded using 100, 512 data points (F1, F2), accumulating 24 scans separated by an interval of 1.5 s. Effective decay rates ($R_{2,eff}$) were extracted from the major resonances using the following formula[22] (Equation 1):

$$R_{2,eff}(\vartheta_{CPMG}) = \frac{-1}{T}\ln\left(\frac{I(\vartheta_{CPMG})}{I_0}\right) \qquad \text{(Equation 1)}$$

Where *T* corresponds to the total transversal relaxation time (40 ms). The spectra of RD experiments were converted to NMRpipe format and processed with the NMRpipe software.[23] This equation was used to obtain the individual exchange contribution (k_{ex}) and the product $\Delta\omega \cdot p_B$ that accounts for the population and the chemical shift of the second state (*B*), which is ultimately related to the amplitude of the motion. The fitting was performed considering each *i* methyl probe separately:

$\Delta\omega_{Hi}$, $\Delta\omega_{Ci}$, k_{exi}, p_{Bi}, $R_{2MQ\infty i}$ ($\chi^2{}_i$)

Where $\Delta\omega$ are the frequency differences between the ^{1}H or ^{13}C resonances of exchanging signals, p_B is the population of the second state, and $R_{2MQ\infty}$ is the effective transverse relaxation at the fast pulsing limit. The global fitting, which considered the same k_{ex} and p_B for all methyl groups, was performed by adjusting the spectral density of RD data by least-squares. The global fitting did not improve the results obtained by the independent one, as revealed by the *F*-test statistical analysis.

The deconvolution of the product $\Delta\omega \cdot p_B$ from a dataset obtained in a single static field was not statistically reliable. For this reason, several replicate fittings were performed in order to evaluate the reliability of the independent fitting. All replicates yielded highly reproducible results, which allowed the extraction of estimated values for $\Delta\omega(^{13}C)$ and p_B separately. ΔR_{ex} values used to depict Figure 3 A were obtained as the difference between the theoretical $R_{2,eff}$ values at the low and the fast-pulsing limit ($R_{2\infty}$). Given the absence of measurable exchange in the RD profiles of POP bound to ZPP and to KYP-2047, fitting was not performed in the case of inhibitor-bound POP.

Online gel filtration coupled to SAXS: HisTag-cleaved samples of free and ZPP-bound POP were subjected to an online Superdex 200 10/300 SEC column coupled to EMBL P12 beamline of the storage ring PETRA III (DESY, Hamburg), using a PILATUS 2M pixel detector (DECTRIS, Switzerland). The column was run at 0.35 ml/min, acquiring 1 frame per second. The X-ray beam wavelength was 1.24 Å, and the range of momentum transfer covered was $0.007 < s < 0.444$ Å^{-1}. The scattering profiles of all frames were inspected, and anomalous profiles were discarded. The scattering profiles corresponding to the pure buffer frames of free and ZPP-bound POP datasets were averaged and subsequently subtracted from all profiles using the PRIMUS program[24] (ATSAS data analysis software). The same program was used to average the subtracted scattering profiles of monomer species of free and inhibited POP, and to derive forward scattering ($I(0)$) and R_g from the Guinier approximation. $P(r)$ distribution functions were obtained with the GNOM program.[25]

Computational methods and ensemble optimization method (EOM): All free POP MD simulations were performed with AMBER12 software.[26] The ff99SB force field[27] for proteins was used, and explicit water molecules were incorporated as TIP3P water model.[28] Protein structures were neutralized and an additional number of sodium and chloride ions were added to simulate physiological saline solution. Protein plus ions were then solvated in pre-equilibrated water molecules in a truncated octahedron box with a 15 Å layer. After energy minimization, temperature was progressively raised to 300°K using constant pressure dynamics. All production runs were done with a time step of 2.0 fs in NPT ensemble (1 bar and 298°K). The shorter MD simulation for ZPP-bound POP was computed using the Desmond molecular dynamics program.[29] The OPLS-AA force field and TIP3P water model were used.[28] The default relaxation protocol in Desmond was used, followed by the production run in the NPT ensemble. Prior to the EOM, theoretical scattering curves were calculated from the simulated PDB files using CRYSOL software (ATSAS data analysis software).[30]

The EOM was performed over a sub-ensemble of *N* structures from a large pool of *M* model structures ($M >> N$) by minimizing the χ^2 between the experimental (I_{exp}) and theoretical (I_{theor}) profiles (Equation 2):

$$\chi^2 = \frac{1}{K-1}\sum_{j=1}^{K}\left[\frac{\mu I_{theor}(s_j) - I_{exp}(s_j)}{\sigma(s_j)}\right]^2 \qquad \text{(Equation 2)}$$

Where *K* is the number of data points, $\sigma(s)$ are the standard deviations, and μ is a scaling factor. $I_{theor,n}(s)$ is defined from the individual *n* profiles as follows (Equation 3):

$$I_{theor}(s) = \frac{1}{N}\sum_{n=1}^{N} I_{theor,n}(s) \qquad \text{(Equation 3)}$$

Experimental curves used in the EOM comprised data points from $s <$ 0.15 Å^{-1} for POP, and from $s <$ 0.3 Å^{-1} for POP bound to ZPP. Constant

subtraction was applied in all cases. The EOM was carried out using 50 random initial sub-ensembles of *N*=20 structures, since the use of more structures in this method (*N* = 50) did not improve the result.[20] A total of 1500 generations were performed. One hundred independent EOM runs were performed, and the most frequent result was taken as the solution with best fit (Figure 4 A).

Acknowledgements

This work was supported by the Institute for Research in Biomedicine, MINECO-FEDER (Bio2013-40716-R, CTQ2013-48287 and CTQ2012-32183/BQU), and the *Generalitat de Catalunya* (XRB and Grup Consolidat 2014SGR521). AL has received funding from the *Instituto de Salud Carlos III*. PB acknowledges the *Agence Nationale de la Recherche* (SPIN-HD-ANR-CHEX-2011) and the ATIP-Avenir program for financial support. FHT's fellowship is co-funded by the INSERM and the University of Copenhagen. Technical assistance from staff at the P12 beam line (EMBL/DESY) is acknowledged.

Keywords: protein dynamics • protein-protein interactions • prolyl oligopeptidase • NMR spectroscopy • SAXS

[1] a) P. Bernado, M. Blackledge, *Nature* **2010**, *468*, 1046-1048; b) K. Henzler-Wildman, D. Kern, *Nature* **2007**, *450*, 964-972.

[2] a) L. Nevola, E. Giralt, *Chemical Communications* **2015**, *51*, 3302-3315; b) S. Jaeger, P. Aloy, *IUBMB Life* **2012**, *64*, 529-537.

[3] D. D. Boehr, R. Nussinov, P. E. Wright, *Nature chemical biology* **2009**, *5*, 789-796.

[4] D. F. Cunningham, B. O'Connor, *The international journal of biochemistry & cell biology* **1998**, *30*, 99-114.

[5] V. Fulop, Z. Bocskei, L. Polgar, *Cell* **1998**, *94*, 161-170.

[6] a) M. Li, C. Chen, D. R. Davies, T. K. Chiu, *The Journal of biological chemistry* **2010**, *285*, 21487-21495; b) L. Shan, Mathews, II, C. Khosla, *Proceedings of the National Academy of Sciences of the United States of America* **2005**, *102*, 3599-3604.

[7] P. Canning, D. Rea, R. E. Morty, V. Fulop, *PloS one* **2013**, *8*, e79349.

[8] N. Kichik, T. Tarrago, B. Claasen, M. Gairi, O. Millet, E. Giralt, *Chembiochem : a European journal of chemical biology* **2011**, *12*, 2737-2739.

[9] K. Kaszuba, T. Rog, R. Danne, P. Canning, V. Fulop, T. Juhasz, Z. Szeltner, J. F. St Pierre, A. Garcia-Horsman, P. T. Mannisto, M. Karttunen, J. Hokkanen, A. Bunker, *Biochimie* **2012**, *94*, 1398-1411.

[10] E. Di Daniel, C. P. Glover, E. Grot, M. K. Chan, T. H. Sanderson, J. H. White, C. L. Ellis, K. T. Gallagher, J. Uney, J. Thomas, P. R. Maycox, A. W. Mudge, *Molecular and cellular neurosciences* **2009**, *41*, 373-382.

[11] a) M. H. Savolainen, X. Yan, T. T. Myohanen, H. J. Huttunen, *The Journal of biological chemistry* **2015**; b) I. Brandt, M. Gérard, K. Sergeant, B. Devreese, V. Baekelandt, K. Augustyns, S. Scharpé, Y. Engelborghs, A.-M. Lambeir, *Peptides* **2008**, *29*, 1472-1478.

[12] J. I. Venalainen, J. A. Garcia-Horsman, M. M. Forsberg, A. Jalkanen, E. A. Wallen, E. M. Jarho, J. A. Christiaans, J. Gynther, P. T. Mannisto, *Biochemical pharmacology* **2006**, *71*, 683-692.

[13] a) T. T. Myohanen, M. J. Hannula, R. Van Elzen, M. Gerard, P. Van Der Veken, J. A. Garcia-Horsman, V. Baekelandt, P. T. Mannisto, A. M. Lambeir, *British journal of pharmacology* **2012**, *166*, 1097-1113; b) M. H. Savolainen, C. T. Richie, B. K. Harvey, P. T. Mannisto, K. A. Maguire-Zeiss, T. T. Myohanen, *Neurobiology of disease* **2014**, *68*, 1-15.

[14] A. G. Palmer Iii, *Chemical Reviews* **2004**, *104*, 3623-3640.

[15] a) H. D. T. Mertens, D. I. Svergun, *Journal of Structural Biology* **2010**, *172*, 128-141; b) D. A. Jacques, J. Trewhella, *Protein Science* **2010**, *19*, 642-657.

[16] D. M. Korzhnev, K. Kloiber, V. Kanelis, V. Tugarinov, L. E. Kay, *Journal of the American Chemical Society* **2004**, *126*, 3964-3973.

[17] a) I. Gelis, A. M. Bonvin, D. Keramisanou, M. Koukaki, G. Gouridis, S. Karamanou, A. Economou, C. G. Kalodimos, *Cell* **2007**, *131*, 756-769; b) T. L. Religa, R. Sprangers, L. E. Kay, *Science* **2010**, *328*, 98-102.

[18] V. Tugarinov, P. M. Hwang, J. E. Ollerenshaw, L. E. Kay, *Journal of the American Chemical Society* **2003**, *125*, 10420-10428.

[19] T. Yoshimoto, K. Kawahara, F. Matsubara, K. Kado, D. Tsuru, *Journal of biochemistry* **1985**, *98*, 975-979.

[20] P. Bernadó, E. Mylonas, M. V. Petoukhov, M. Blackledge, D. I. Svergun, *Journal of the American Chemical Society* **2007**, *129*, 5656-5664.

[21] T. Tarragó, S. Frutos, R. A. Rodriguez-Mias, E. Giralt, *Chembiochem : a European journal of chemical biology* **2006**, *7*, 827-833.

[22] F. A. A. Mulder, N. R. Skrynnikov, B. Hon, F. W. Dahlquist, L. E. Kay, *Journal of the American Chemical Society* **2001**, *123*, 967-975.

[23] F. Delaglio, S. Grzesiek, G. W. Vuister, G. Zhu, J. Pfeifer, A. Bax, *Journal of biomolecular NMR* **1995**, *6*, 277-293.

[24] P. V. Konarev, V. V. Volkov, A. V. Sokolova, M. H. J. Koch, D. I. Svergun, *Journal of Applied Crystallography* **2003**, *36*, 1277-1282.

[25] D. Svergun, *Journal of Applied Crystallography* **1992**, *25*, 495-503.

[26] D. A. Case, T. A. Darden, T. E. Cheatham Iii, C. L. Simmerling, J. Wang, R. E. Duke, R. Luo, R. C. Walker, W. Zhang, K. M. Merz, B. Roberts, S. Hayik, A. Roitberg, G. Seabra, J. Swails, A. W. Götz, I. Kolossváry, K. F. Wong, F. Paesani, J. Vanicek, R. M. Wolf, J. Liu, X. Wu, S. R. Brozell, T. Steinbrecher, H. Gohlke, Q. Cai, X. Ye, J. Wang, M. J. Hsieh, G. Cui, D. R. Roe, D. H. Mathews, M. G. Seetin, R. Salomon-Ferrer, C. Sagui, V. Babin, T. Luchko, S. Gusarov, A. Kovalenko, P. A. Kollman, **2012**.

[27] V. Hornak, R. Abel, A. Okur, B. Strockbine, A. Roitberg, C. Simmerling, *Proteins* **2006**, *65*, 712-725.

[28] W. L. Jorgensen, J. Chandrasekhar, J. D. Madura, R. W. Impey, M. L. Klein, *The Journal of Chemical Physics* **1983**, *79*, 926-935.

[29] N. Y. D. E. Shaw Research, *Desmond Molecular Dynamics System, version 3.1* **2012**.

[30] D. Svergun, C. Barberato, M. H. J. Koch, *Journal of Applied Crystallography* **1995**, *28*, 768-773.

Entry for the Table of Contents

COMMUNICATION

A spoke on the wheels: A combined approach based on NMR and SAXS experiments complemented by MD simulations has shown that active site-directed inhibitors of prolyl oligopeptidase (POP, 81 KDa) abolishes a pre-existing open/close conformational equilibrium. Probably, abolishing conformational dynamics by inhibitors causes significant alterations on the molecular recognition events of POP.

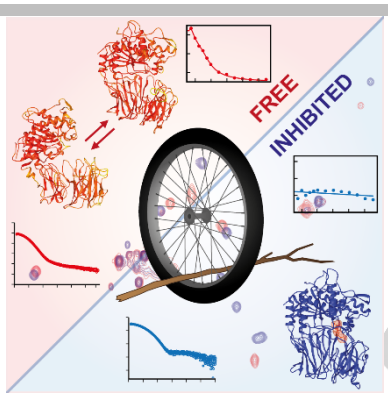

*Abraham López, Fátima Herranz-Trillo, Martin Kotev, Margarida Gairí, Víctor Guallar, Pau Bernadó, Oscar Millet, Teresa Tarragó, and Ernest Giralt**

Page No. – Page No.
Active Site-Directed Inhibitors of Prolyl Oligopeptidase Abolishes its Conformational Dynamics